6

Barbara Horvat, Vilma Ducman

Influence of curing/drying methods including microwave heating on alkali activation of waste casting cores

INFLUENCE OF CURING/DRYING METHODS INCLUDING MICROWAVE HEATING ON ALKALI ACTIVATION OF WASTE CASTING CORES

B. Horvat[1], V. Ducman[2]

[1,2] Slovenian Nationa Building and Civil Engineering Institute, Department of Materials
Dimičeva ul. 12, 1000 Ljubljana
e-mail: barbara.horvat@zag.si, vilma.ducman@zag.si

SUMMARY: Within previous investigation alkali activation of waste casting cores at room temperature did not give promising results, i.e. when the precursor was gently ground and sieved below 600 µm the alkali activated material fell apart at demolding, and when the precursor was ground below 90 µm, the alkali activated material did not solidify in more than 2 years. , Therefore different drying/curing methods were applied to enhance the reaction. Waste casting cores were prepared in two granulations (sieved below 600 µm and below 90 µm), activated with Na-water glass and 10 M NaOH, cured at different temperatures (70 °C and room temperature), and subsequently cured/dried at three different conditions: room temperature, 110 °C, and irradiated with microwaves. The highest compressive strength, 25 MPa, was gained with subsequent curing/drying at 110 °C. The lowest density, 0.5 kg/l, with compressive strength above 3 MPa, was achieved with subsequent curing/drying with microwaves.

KEYWORDS: Waste casting cores; Alkali activation; Curing; Drying; Microwaves; Mechanical strength.

1 INTRODUCTION

Alkali activated materials (AAM) can be produced from different waste materials containing enough Si and Al in the amorphous phase, which react with alkalis and form an aluminosilicate network (ASN) of SiO4 and AlO4 tetrahedrons that are joined by oxygen bridges. In the network, the negative charge localized on Al^{3+} is compensated with positive ions from alkali liquid [1]. Most researched precursors for alkali activation are metakaolin [2], fly-ash [3], slag [2] and their mixtures [2]. The technology was proved also in praxis:

- airport runway in Brisbane, Australia [4], where for precursors blast furnace slag and fly-ash were used,
- 4-floor public house (University of Queensland's Global Change Institute) in Queensland, Australia [5], where floors are made from 33 precast panels that are made from slag and fly ash-based geopolymer concrete.

Alkali activated foams (AAF) represent added value to the alkali activated materials, as being porous, lightweight with the potential to be used as fire-resistant thermal and/or acoustic insulators [6]. Porosity can be achieved with several methods:

- mechanical process using preformed air bubbles [6],
- chemical reaction of foaming agents (Na-perborate, Na-lauryl sulphate, Al powder, H_2O_2, metal silica impurities contained in silica fumes etc.) with alkali activated slurry of precursor and source of alkali, where gases are formed and trapped in the liquid network [7],
- chemical reactions of ingredients present in the precursor(s) with alkali and/or alkali glass, i.e. self-foaming [8],
- removal of hydrated water from alkali activated material with temperature [9],
- replica method with removal (combustion, decomposition) of "sacrificed" material like organic compounds, plastic, carbon, sulphate [10],
- bloating of the precursor at high temperatures [11],
- etc.

Casting cores which are also the subject of the present paper, are commonly produced with three different methods: coldbox (binder hardens sand with chemical reaction without addition of thermal energy [12]), hotbox (binder hardens sand with heat [12]) and warmbox/shellbox (binder in the outer layer of sand core hardens with heat [13]). Binders can be inorganic like alkali glass, cement, clay, bentonite, which are gas emission-free, or organic like furan, phenolic urethane, phenol-formaldehyde resin, which lead to emission of health-hazardous gasses during exposure to casting metal [14].

Drying is an important part of the core preparation process. Common drying method with implementing heat in a

furnace is just surface drying [15], drying with the use of gasses in casting core production is semi-volumetric (depending on if the gas is only around the core or blown through tubes into the core, depending on the viscosity of the fluid [16]), while drying with microwaves is volumetric [15]. When drying with the surface method, samples are dried to a certain depth of the bulk sample, which depends on the temperature applied and time on the temperature, while volumetric drying is drying throughout the whole bulk's volume at the same time in short(er) time [15] where high(er) temperatures can take place [17] that can also change the mineralogical composition, size of grains, which makes procedure useful also for (pre)sintering of ceramics [18]. The volumetric drying is a consequence of dielectric polarization of molecules with electromagnetic irradiation [19] with wavelengths from 1 mm to 1 m, frequency 300 GHz to 300 MHz respectively [20].

A newer emission-free warm-box method is where microwaves are used for heating to harden the binder consisting of alkali glass and alkali on the surface of quartz sand (which is not alkali activated synthesis, just binding of quartz sand into a mould). Results of all research available so far are showing that using microwave technology gives better strength and uses less energy than alternatives [12], therefore the use of microwave irradiation in connection to the alkali activated synthesis using waste casting cores might contribute to increase of mechanical properties too.

In the present study shell-box casting cores were prepared in 2 different granulation, 3 different alkali activating mixtures and with 3 different drying procedures to assess the influence of drying/curing methods on properties of final AAM, and to thus determine optimal preparation method.

2 MATERIALS AND METHODS

2.1 Analysis of precursor

Waste casting cores (WCC) from company Termit d.d. (Drtija, Slovenia), labelled 10 09 06 (according to the Classification list of waste from Official Gazette of the Republic of Slovenia, no. 20/01 Annex 1), used in the study are shell-box cores that could not be further used due to the damage in the factory.

X-ray fluorescence on melted discs (XRF; Thermo Scientific ARL Perform'X Sequential XRF) and X-ray powder diffraction (XRD; Empyrean PANalytical X-ray Diffractometer, Cu X-Ray source) analysis were performed with material dried at 70 °C for 24 h (WTB Binder), ground with the vibrating disk mill (Siebtechnik) and sieved below 90 µm. XRF analysis was done with software UniQuant 5, XRD analysis with X'Pert Highscore plus 4.1. Rietveld refinement using external standard (a pure crystal of Al_2O_3) was implemented on XRD pattern to estimate the amount of amorphous phase and minerals present in waste casting cores.

Fourier-transform infrared spectroscopy (FTIR; PerkinElmer Spectrum Two) was performed on a sample that was ground with the vibrating disk mill and sieved below 90 µm.

Scanning electron microscopy (SEM; Jeol JSM-IT500) investigation was performed under high vacuum conditions on dried samples.

2.2 Preparation of alkali activated samples

Waste casting cores were dried at 70 °C for 24 h, ground with a pestle and mortar and sieved below 600 µm, or ground in a vibrating disk mill and sieved below 90 µm.

Alkali activation was performed by addition of 10 M NaOH (Donau Chemie Ätznatron Schuppen, EINECS 215-785-5) to Na-water glass (Geosil, 344/7, Woelner) in equal mass amounts. Liquids were stirred until the mixture became clear, and then poured into the sample in mass ratio "waste material : alkali : alkali glass" 2.5:1:1 (if not stated otherwise) under constant mixing for 1 min. The slurry was poured into plastic moulds of dimensions 25x12x12 mm3, cured at 70 °C for 24 h, demoulded, subsequently cured (because curing at 70 °C for 24 h was not enough) at room temperature, with kitchen microwave (Gorenje Microwave oven MO 17DV, 2.45 GHz, 700 W) for different times or until the sample was completely dry, or in drying chamber at 110 °C for 24 h (WTB Binder).

2.3 Analysis of AAM

Measurement of compressive strength of alkali activated casting cores was performed with compressive and bending strength testing machine (ToniTechnik ToniNORM) 1 month after solidification.

Density was determined by weighting the sample and dividing its mass with geometrically determined volume.

Fourier-transform infrared spectroscopy (FTIR; PerkinElmer Spectrum Two) was performed on alkali activated sample which was dried with different methods.

The surface and microstructure of selected samples were investigated with the scanning electron microscope (SEM; Jeol JSM-IT500) under high vacuum conditions.

3 RESULTS AND DISCUSSION

3.1 Analysis of precursor

SEM micrographs of WCC ground in a mortar with pestle and waste casting cores ground in vibrating disk mill are presented in Figure 1 (a) and (b) respectively. Precursor sieved below 600 µm (a) consists of particles with smooth edges, smooth surface and sizes generally above 100 µm, while precursor sieved below 90 µm (b) is powder-like consisting of particles with sharp edges and smooth surface. The damaged surface is seen already on particles of precursor gently ground and sieved below 600 µm (red circle in Figure 1 (a)), which is a consequence of destroying linking bridges connected with the sand base [21].

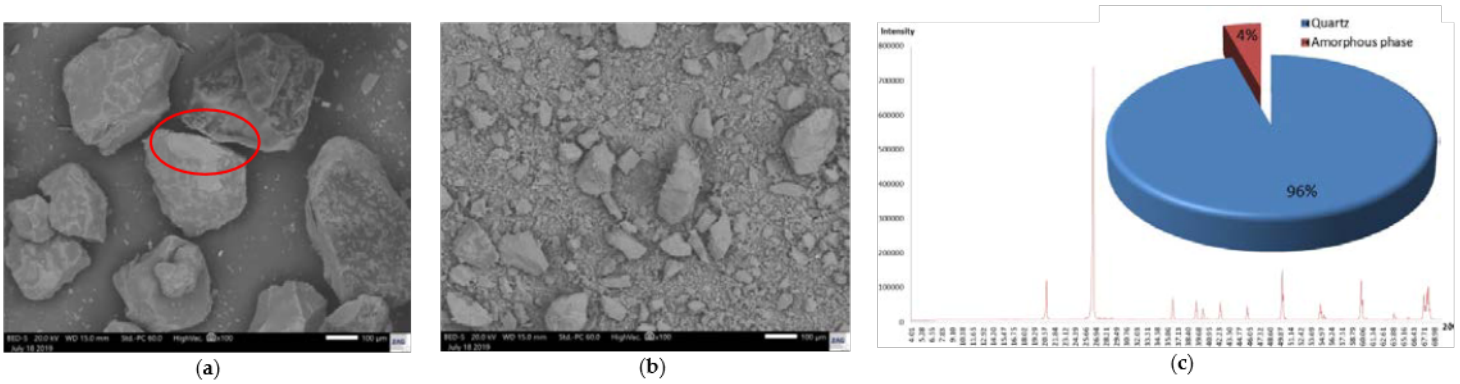

(a) (b) (c)

Figure 1: SEM micrographs of WCC. (a) Gently ground in a mortar with pestle and sieved below 600 µm (red circle: damaged surface); (b) ground in vibrating disk mill and sieved below 90 µm, (c) XRD pattern of WCC and on the inset its Rietveld refinement.

Chemical analysis was performed by means of XRF. It showed that there is a small mass percentage of K (0.09%), Ca (0.10%) and Al (1.33%), while Si is in aboundance (44.60%). With Rietveld refinement performed on XRD pattern (see Figure 1 (c)) the mass percentage of crystalline and amorphous phase was estimated. Only quartz (96%) was found to be in crystalline phase, meaning that there is only a small amount of Al, K and Mg in precursor useful for alkali activation.

Determination of the presence of an organic compound in WCC was performed utilizing FTIR, which is presented in Figure 2. Frequency 2980 cm^{-1} corresponds to C-H values of alkyl groups (orange vertical line in Figure 2) [22], frequencies around 1450 cm^{-1} correspond to C-H_2 and C-H_3 bendings from aromatic ring (phenol from the phenol-formaldehyde resin used in casting core production, purple vertical lines in Figure 2) [23], frequencies 3340 cm^{-1} and 1635 cm^{-1} correspond to O-H in water (blue vertical lines in Figure 2) [24], while Si-O bonds are from 950 to 1110 cm^{-1}, Si-O from quartz around 800 cm^{-1} [25].

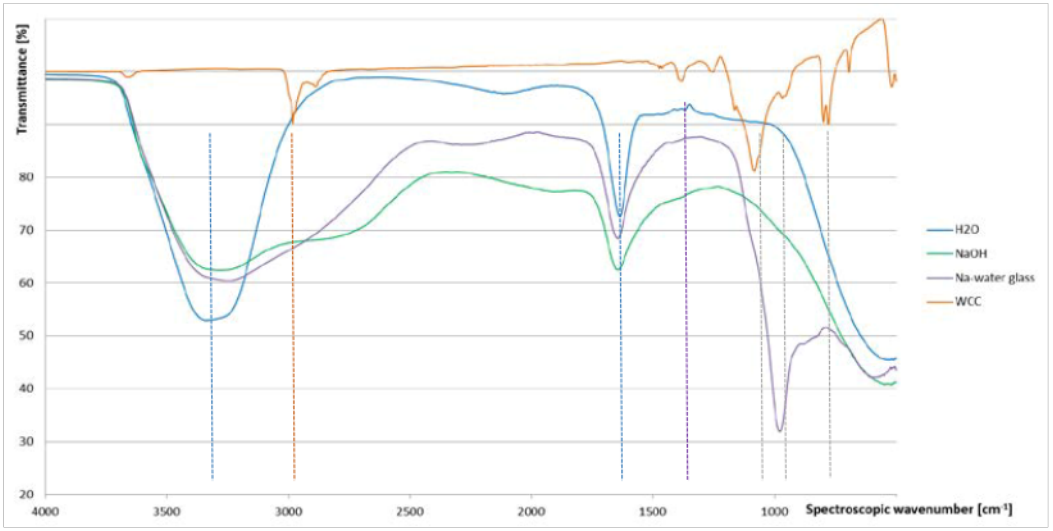

Figure 2: FTIR of all ingredients used in alkali activation. Dashed blue lines O-H bonds, dashed orange lines C-H bonds, dashed purple lines aromatic C-H_2 and C-H_3 bonds, dashed grey lines Si-O bonds.

3.2 Analysis of bulk AAM

Compressive strength and density are presented in Table 1 and vary according to the preparation of the precursor (degree of milling), ratio precursor : 10 M NaOH : Na-water glass, and drying method. From the results given in Table 1, it can be concluded that:

- to achieve higher mechanical properties, it is better that precursor is ground and sieved below 90 µm (smaller particles, more surface), otherwise, the experiment is not successful,
- in case of bigger particles of the precursor amount of liquid phase is crucial, i.e. if there is not enough liquid phase, successful demolding is not possible,
- in case of smaller particles of the precursor amount of liquid phase has to be low enough to gain higher final compressive strength, at least when using surface drying method,
- the highest influence on final properties has used the method of subsequent curing/drying:
- if samples were subsequently cured/dried on mild conditions (room conditions, RC), AAM did not even solidify in more than 2 years,
- if samples were subsequently cured/dried with surface drying at 110 °C, density was comparable or lower to samples dried at RC, but samples did solidify and had compressive strength up to 25 MPa when particles of the precursor were smaller,
- if samples were subsequently cured/dried with volumetric drying method (microwaves), AAM solidified in the shortest time, density lowered, as well as compressive strength if particles of precursor were smaller, i.e. there was no difference in compressive strength when volumetric or surface drying at 110 °C were performed on AMM synthesized from precursor consisting of bigger particles,
- density and compressive strength showed time dependence on irradiation with microwaves presented also in Figure 3.

Table 1: Compressive strength and density of prepared AAM. RC = room conditions, MW = microwave.

Preparation of precursor	Precursor : 10M NaOH : Na-water glass	Curing conditions	Subsequent drying method	Density [kg/l]	Compressive strength [MPa]
< 600 µm	3.75 : 1 : 1	70 °C 24 h	RC	*	
< 600 µm	3.3 : 1 : 1	70 °C 24 h	RC		
< 600 µm	2.5 : 1 : 1	70 °C 24 h	RC	1.60	Does not solidify
< 600 µm	2.5 : 1 : 1	70 °C 24 h	110 °C 24 h	1.55	17.61
< 600 µm	2.5 : 1 : 1	70 °C 24 h	MW 0.66 min	1.49	17.55
< 90 µm	3.3 : 1 : 1	70 °C 24 h	RC	1.62	Does not solidify
< 90 µm	3.3 : 1 : 1	70 °C 24 h	110 °C 24 h	1.60	24.98
< 90 µm	3.3 : 1 : 1	70 °C 24 h	MW 0.66 min	1.20	5.55
< 90 µm	2.5 : 1 : 1	70 °C 24 h	RC	1.64	Does not solidify
< 90 µm	2.5 : 1 : 1	70 °C 24 h	110 °C 24 h	1.03	11.42
< 90 µm	2.5 : 1 : 1	70 °C 24 h	MW 0.08 min	1.46	0.25
< 90 µm	2.5 : 1 : 1	70 °C 24 h	MV 0.17 min	1.46	0.34
< 90 µm	2.5 : 1 : 1	70 °C 24 h	MV 0.33 min	1.24	0.77
< 90 µm	2.5 : 1 : 1	70 °C 24 h	MV 0.5 min	0.94	0.78
< 90 µm	2.5 : 1 : 1	70 °C 24 h	MW 0.66 min	0.90	5.71
< 90 µm	2.5 : 1 : 1	70 °C 24 h	MW 0.83 min	0.71	2.90
< 90 µm	2.5 : 1 : 1	70 °C 24 h	MW 1 min	0.73	2.70
< 90 µm	2.5 : 1 : 1	70 °C 24 h	MW 1.17 min	0.78	2.86
< 90 µm	2.5 : 1 : 1	70 °C 24 h	MW 1.5 min	0.59	2.10
< 90 µm	2.5 : 1 : 1	70 °C 24 h	MW 2 min	0.70	2.26
< 90 µm	2.5 : 1 : 1	70 °C 24 h	MW 3 min	0.64	1.95
< 90 µm	2.5 : 1 : 1	70 °C 24 h	MW 4 min	0.72	1.90
< 90 µm	2.5 : 1 : 1	70 °C 24 h	MW 5 min	0.72	1.07

* = not solidified

Dependence of time irradiation with microwaves on density and compressive strength of sample prepared from precursor ground in vibrating disk mill and sieved below 90 µm, mixed with 10 M NaOH and Na-water glass in ratio 2.5:1:1 respectively, are presented in Figure 3. Density lowers with an early time of irradiation and reaches an approximately constant value. Compressive strength starts increasing with irradiation, reaches peak soon (sample is completely dried) and starts slower decline (melting).

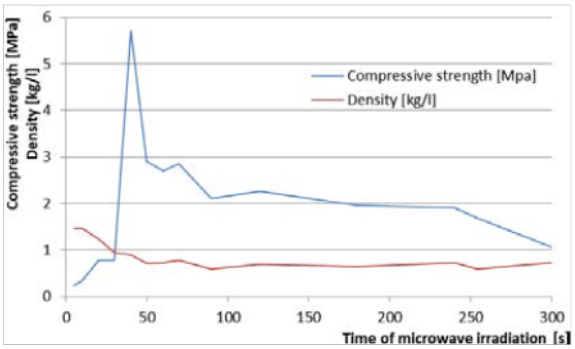

Figure 3: Compressive strength and density of samples prepared from precursor ground in vibrating disk mill and sieved below 90 µm, mixed with 10 M NaOH and Na-water glass in ratio 2.5:1:1 respectively, in the dependence of irradiation with microwaves for a different amount of time.

Beside weak solidification at milder curing conditions (70 °C) and difficulties at demolding (shape of the prism was easily damaged after primary curing, AAM reacted with glass surface when subsequently curried/dried at 110 °C), there was no shrinkage noticed. However, when the precursor used was from smaller particles (sieved below 90 µm), foaming was noticed as can be seen on SEM micrographs in Figure 4 to Figure 6, which were performed on last four AAM presented in Table 2, where the difference in the preparation of AAM is only the method of drying. AAM dried at room conditions had the spherical shape of pores (Figure 4 (a)) that measured in average 265.5 µm in diameter (standard deviation is 94.3 µm, maximal diameter found under SEM was 471.4 µm). Pores of AAM dried at 110 °C lost the spherical shape (Figure 5 (a)) and became bigger due to coalescence of pores, i.e. average SEM diameter was 281.8 µm (standard deviation is 172.7 µm, maximal diameter found under SEM was 858.2 µm). Pores of AAM dried with microwaves for 0.66 min also lost the spherical shape (Figure 6 (a)) and got even bigger, i.e. average SEM diameter was 485.2 µm (standard deviation is 261.3 µm, maximal diameter found under SEM was 1109 µm).

EDXS mappings in Figures 4 to Figure 6 (1st EDXS row) are performed on 1000-times magnified micrographs (Figure 5 to Figure 6 (b)). On all EDXS mappings, it is clear, that Al, Si and Na, important in alkali activation, are not uniformly distributed. The intensity of C compared to the intensity of other elements on EDXS is stronger on sample dried at room temperatures, compared to intensity when the sample was dried at 110 °C, and with microwaves. The intensity of O is comparable to Na when the sample was dried at room conditions. With drying at 110 °C the intensity of O increases also to the part where Si is detected but is still less intensive compared to sample dried with microwaves, where the intensity of O is the same where Na and Si are detected. The conclusion from these results is that organic compound blocks reaction of alkali and non-organic part of precursor, which is presented on EDXS in Figure 6 performed on the part marked with a red square, where Na and Si are separated (Na represent the envelope of Si), O is present in both areas (where Si and Al were detected).

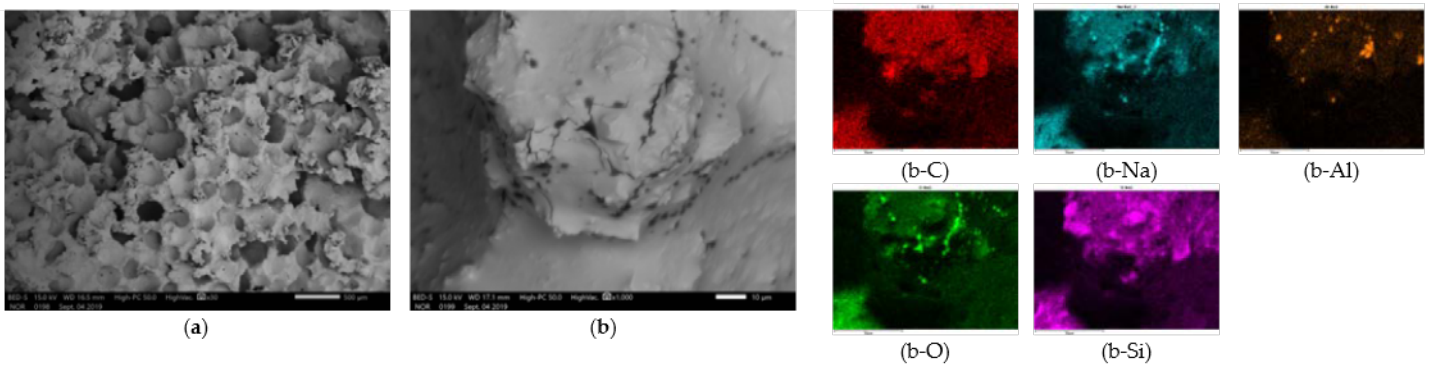

Figure 4: SEM micrographs of AAM, which was prepared from precursor sieved below 90 µm and alkali activated in ratio precursor : 10 M NaOH : Na-water glass = 2.5 :1 :1, dried at room conditions. Magnification (a) 30, (b) 1000. (b-chemical element) EDXS mapping on (b) of the detected chemical element.

In Figure 4 (b), Figure 5 (b) and Figure 6 (b) "matrix" of alkali activated material is presented, which is smooth when dried at room conditions (Figure 4 (b)), and becomes rough with harsher drying conditions (Figure 5 (b) and Figure 6 (b)), where unreacted non-organic part of precursor starts to appear.

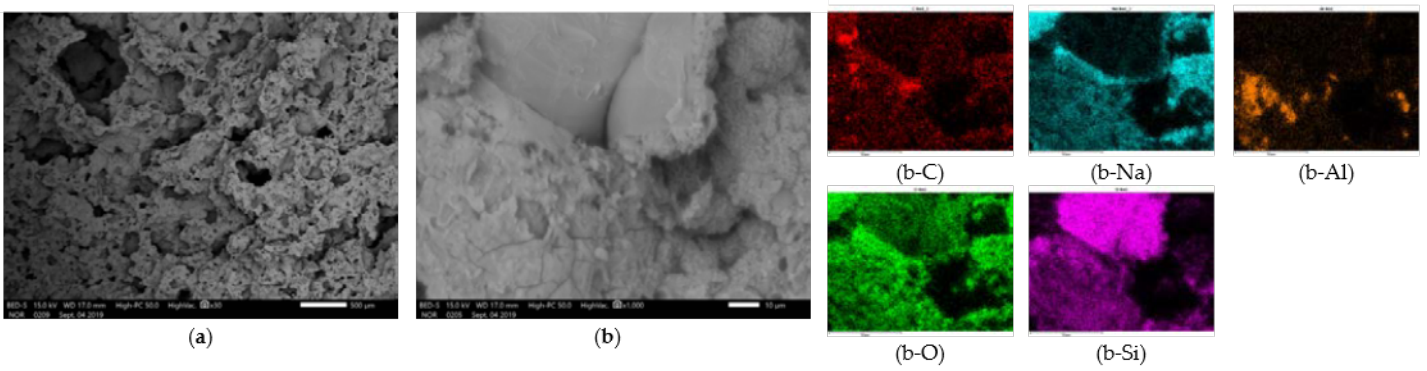

Figure 5: SEM micrographs of AAM, which was prepared from precursor sieved below 90 μm and alkali activated in ratio precursor : 10 M NaOH : Na-water glass = 2.5 :1 :1, dried at 110 °C. Magnification (a) 30, (b) 1000. (b-chemical element) EDXS mapping on (b) of the detected chemical element.

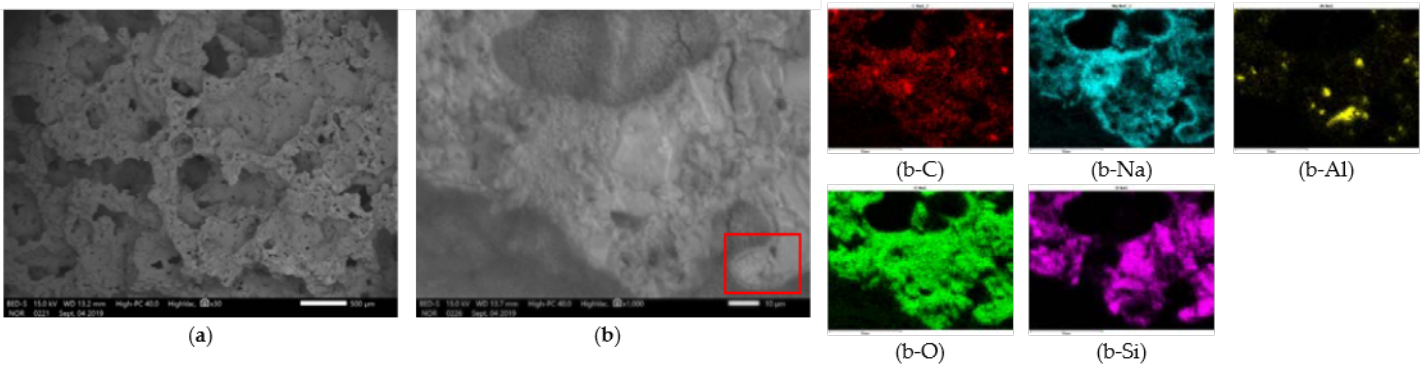

Figure 6: SEM micrographs of AAM, which was prepared from precursor sieved below 90 μm and alkali activated in ratio precursor : 10 M NaOH : Na-water glass = 2.5 :1 :1, dried with microwaves for 0.66 min. Magnification (a) 30, (b) 1000. (b-chemical element) EDXS mapping per chemical element of the area (b).

The foaming process starts with the addition of alkali to precursor and is a consequence of degradation of organic compound present in the precursor: C-H bonds are present only in the precursor as can be seen in Figure 7. FTIR on sample dried at room temperature could be “hiding” the C-H peak of alkyl groups in the wide O-H peak arising from water, which disappears in solidified samples dried at 110 °C and with microwaves.

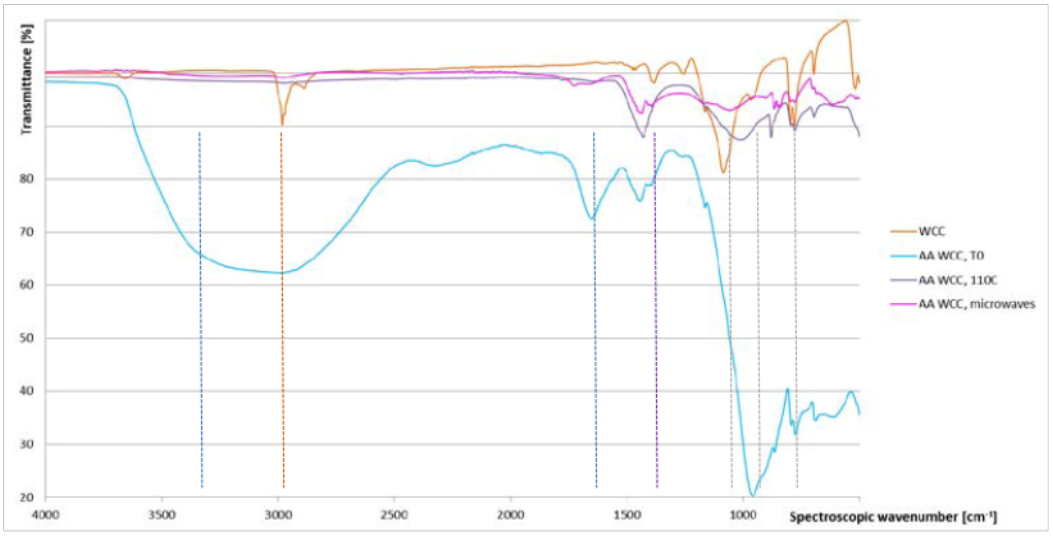

Figure 7: FTIR of precursor and AAM dried with different methods. Blue lines O-H bonds, orange lines C-H bonds, dashed purple lines aromatic C-H_2 and C-H_3 bond, grey lines Si-O bonds.

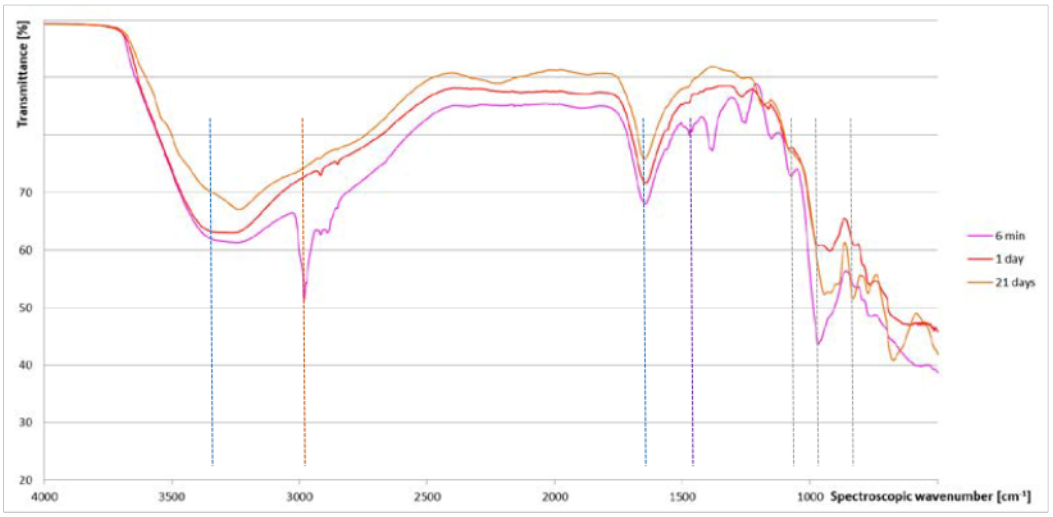

Figure 8: FTIR time dependence of AAM dried at room temperature. Blue lines O-H bonds, orange lines C-H bonds, dashed purple lines aromatic C-H_2 and C-H_3 bonds, grey lines Si-O bonds.

Time dependence of C-H peak from alkyl groups was followed with FTIR from the early time of alkali activation. Peak started to disappear in "O-H peak" with time after the addition of alkali, as is seen in Figure 8. Peak disappearing was accompanied by a foaming process that was not present in a sample without a clear C-H peak.

Time dependence of drying/curing of alkali activated WCC (pre-cured at 70 °C for 24 h) with microwave radiation is presented in Figure 9 and compared to the sample cured for 1 h at room temperature (early stages of curing of alkali activated material) and to the sample cured at 70 °C for 24 h. C-H peak (orange line) and O-H peak "merge" and decrease with time of microwave irradiation, i.e. samples radiated for at least 50 s lose the intense smell (merged peak) and water (the peak at 1635 cm^{-1} disappears). However, the highest compressive strength has the sample irradiated for 40 s (green line in Figure 9) according to Figure 3.

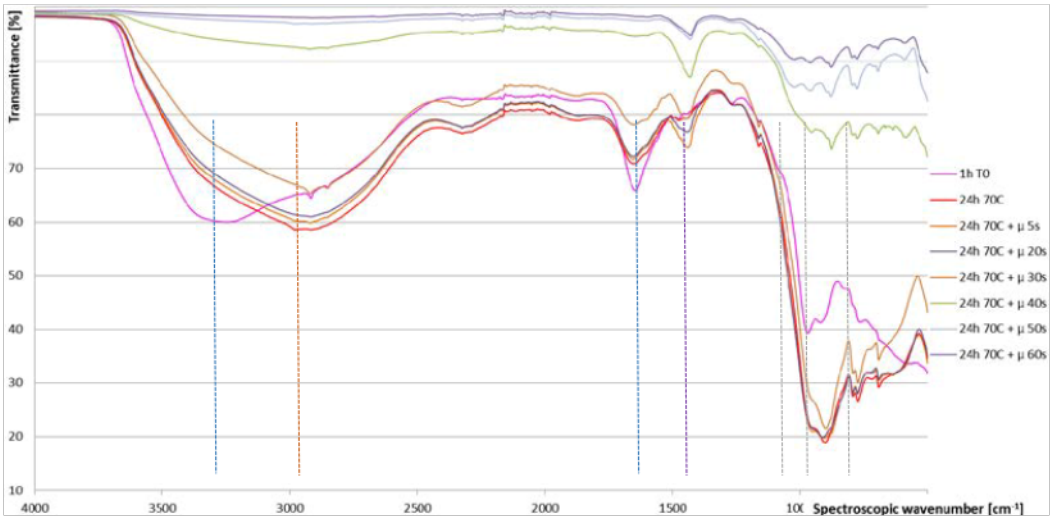

Figure 9: FTIR of AAM dried for 1 h at room temperature and at 70 °C for 24 h without and with additional irradiation with microwaves for different times. Dashed blue lines represent O-H bonds, dashed orange lines C-H bonds, dashed purple lines aromatic C-H_2 and C-H_3 bonds, dashed grey lines Si-O bonds.

4 CONCLUSIONS

Chemical and mineralogical analyses of waste casting cores were performed, AAM was synthesized, their density and compressive strength were determined, and chemical bonds were followed to determine the influence of different drying methods.

It was shown that waste casting cores can be used as a precursor in alkali activation if drying methods are performed under harsher conditions:

- AAM prepared from waste casting cores sieved below 600 µm did not bind good enough to withhold its own mass at demolding, if mass ratio "waste material : alkali : alkali glass" was higher from 2.5:1:1, and if not dried at 110 °C for 24 h or in the microwave. Drying did not have a high impact on density and both methods resulted in a similar value of compressive strength;
- AAM prepared from waste casting cores sieved below 90 µm foamed, was rubber-like and wet for already more than 2 years, unless dried at 110 °C for 24 h or with microwaves. Compressive strength and density showed dependence on the drying procedure, i.e. lower density and lower strength were reached with drying with microwaves. Dependence on mass ratio "waste material : alkali : alkali glass" was also observed, i.e. more liquid phase resulted in lower density and lower compressive strength;
- Compressive strength and density of AAM showed dependence on time of irradiation with microwaves, i.e. highest peak being when water and organic compound are almost removed, which was in our case 40 seconds.

According to FTIR self-foaming was a consequence of the degradation of the organic compound, present in the precursor, in alkali media. The pore size in self-foamed samples showed dependence on drying procedure, i.e. with harsher conditions of drying pores were bigger and less uniform in shape due to coalescence of pores.

Self-foaming was not noticed when precursors used was from bigger particles, probably because of larger empty space between bigger particles that do not react with alkali, so escape of gas from the slurry was easier (into the empty space).

Material solidified and dried only under harsher drying conditions and was accompanied by a change of the matrix' surface from smooth to rough with clearly visible quartz particles from a ground precursor in it. Change of the matrix is according to FTIR and EDXS consequence of the removal of an organic compound.

According to EDXS analysis, common ASN did not form since areas of Al and Si were dislocated, and Na was present mostly on the surface of quartz (Si) particles.

ACKNOWLEDGMENTS

The involvement of V. Ducman was supported by the Slovenian Research Agency Programme Group P2-0273. Cooperation with Termit d.d. and Mrs Alenka Sešek Pavlin from Termit d.d.is highly appreciated.

REFERENCES

[1] F. Škvára, Alkali Activated Material - Geopolymer, (2007) 16.
[2] M.C. Bignozzi, S. Manzi, I. Lancellotti, E. Kamseu, L. Barbieri, C. Leonelli, Mix-design and characterization of alkali activated materials based on metakaolin and ladle slag, Applied Clay Science. 73 (2013) 78–85. https://doi.org/10.1016/j.clay.2012.09.015.
[3] J. Němeček, V. Šmilauer, L. Kopecký, Nanoindentation characteristics of alkali-activated aluminosilicate materials, Cement and Concrete Composites. 33 (2011) 163–170. https://doi.org/10.1016/j.cemconcomp.2010.10.005.
[4] T. Glasby, J. Day, R. Genrich, D.J. Aldred, EFC Geopolymer Concrete Aircraft Pavements at Brisbane West Wellcamp Airport, (2015) 9.
[5] HASSELL | Project - University of Queensland Global Change Institute, HASSELL Studio. (n.d.). https://www.hassellstudio.com/en/cms-projects/detail/the-university-of-queensland-global-change-institute/ (accessed November 13, 2019).
[6] A. Hajimohammadi, T. Ngo, P. Mendis, A. Kashani, J.S.J. van Deventer, Alkali activated slag foams: The effect of the alkali reaction on foam characteristics, Journal of Cleaner Production. 147 (2017) 330–339. https://doi.org/10.1016/j.jclepro.2017.01.134.
[7] A. Hajimohammadi, T. Ngo, P. Mendis, J. Sanjayan, Regulating the chemical foaming reaction to control the porosity of geopolymer foams, Materials & Design. 120 (2017) 255–265. https://doi.org/10.1016/j.matdes.2017.02.026.
[8] Burkhard Walther, Bernhard Feichtenschlager, Shengzhong Zhou, Self-foaming Geopolymer Composition COntaining Aluminum Dross, US 9,580,356 B2, 2017.
[9] R.A. Fletcher, K.J.D. MacKenzie, C.L. Nicholson, S. Shimada, The composition range of aluminosilicate geopolymers, Journal of the European Ceramic Society. 25 (2005) 1471–1477. https://doi.org/10.1016/j.jeurceramsoc.2004.06.001.
[10] A. Rincón Romero, N. Toniolo, A. Boccaccini, E. Bernardo, Glass-Ceramic Foams from 'Weak Alkali Activation' and Gel-Casting of Waste Glass/Fly Ash Mixtures, Materials. 12 (2019) 588. https://doi.org/10.3390/ma12040588.
[11] Y.-L. Wei, S.-H. Cheng, G.-W. Ko, Effect of waste glass addition on lightweight aggregates prepared from F-class coal fly ash, Construction and Building Materials. 112 (2016) 773–782. https://doi.org/10.1016/j.conbuildmat.2016.02.147.
[12] G.S. Cole, Microwave Core Process, 4331197, n.d..
[13] Shell Mold Casting, (n.d.). https://thelibraryofmanufacturing.com/shell_mold_casting.html (accessed November 14, 2019).
[14] F. Czerwinski, M. Mir, W. Kasprzak, Application of cores and binders in metalcasting, International Journal of Cast Metals Research. 28 (2015) 129–139. https://doi.org/10.1179/1743133614Y.0000000140.
[15] L. Punathil, T. Basak, Microwave Processing of Frozen and Packaged Food Materials: Experimental, in: Reference Module in

Food Science, Elsevier, 2016. https://doi.org/10.1016/B978-0-08-100596-5.21009-3.
[16] D.S. Deore, G.B. Chaudhari, A.G. Chaturvedi, S.U. Gunjal, A studay of core and its types for casting process, (2015) 11.
[17] D. Agrawal, Microwave sintering of metal powders, in: Advances in Powder Metallurgy, Elsevier, 2013: pp. 361–379. https://doi.org/10.1533/9780857098900.3.361.
[18] M. Willert-Porada, Simultaneous use of different high frequency energy sources for material processing, in: Novel Materials Processing by Advanced Electromagnetic Energy Sources, Elsevier, 2005: pp. 99–104. https://doi.org/10.1016/B978-008044504-5/50020-9.
[19] M. Stachowicz, K. Granat, D. Nowak, Application of microwaves for innovative hardening of environment-friendly water-glass moulding sands used in manufacture of cast-steel castings, Archives of Civil and Mechanical Engineering. 11 (2011) 209–219. https://doi.org/10.1016/S1644-9665(12)60184-8.
[20] R.T. Hitchcock, Radio-frequency and microwave radiation, 3rd ed, American Industrial Hygiene Association, Fairfax, Va, 2004.
[21] M. Stachowicz, K. Granat, Ł. Pałyga, Effect of Sand Wetting on Physically Hardened Moulding Sands Containing a Selected Inorganic Binder. Part 2, Archives of Foundry Engineering. 16 (2016) 79–84. https://doi.org/10.1515/afe-2016-0007.
[22] H.S. Mansur, C.M. Sadahira, A.N. Souza, A.A.P. Mansur, FTIR spectroscopy characterization of poly (vinyl alcohol) hydrogel with different hydrolysis degree and chemically crosslinked with glutaraldehyde, Materials Science and Engineering: C. 28 (2008) 539–548. https://doi.org/10.1016/j.msec.2007.10.088.
[23] Y. Chen, C. Zou, M. Mastalerz, S. Hu, C. Gasaway, X. Tao, Applications of Micro-Fourier Transform Infrared Spectroscopy (FTIR) in the Geological Sciences—A Review, International Journal of Molecular Sciences. 16 (2015) 30223–30250. https://doi.org/10.3390/ijms161226227.
[24] B.L. Mojet, S.D. Ebbesen, L. Lefferts, Light at the interface: the potential of attenuated total reflection infrared spectroscopy for understanding heterogeneous catalysis in water, Chemical Society Reviews. 39 (2010) 4643. https://doi.org/10.1039/c0cs00014k.
[25] M. Pavlin, B. Horvat, A. Frankovič, V. Ducman, Mechanical, microstructural and mineralogical evaluation of alkali-activated waste glass and stone wool, Ceramics International. (2021) S0272884221004168. https://doi.org/10.1016/j.ceramint.2021.02.068.